



**HAL**  
open science

## Iron deposition on multi-walled carbon nanotubes by fluidized bed MOCVD for aeronautic applications

Pierre Lassègue, Laure Noé, Marc Monthieux, Brigitte Caussat

### ► To cite this version:

Pierre Lassègue, Laure Noé, Marc Monthieux, Brigitte Caussat. Iron deposition on multi-walled carbon nanotubes by fluidized bed MOCVD for aeronautic applications. *physica status solidi (c)*, 2015, 12 (7), pp.861-868. 10.1002/pssc.201510036 . hal-01758088

**HAL Id: hal-01758088**

**<https://hal.science/hal-01758088>**

Submitted on 9 Dec 2023

**HAL** is a multi-disciplinary open access archive for the deposit and dissemination of scientific research documents, whether they are published or not. The documents may come from teaching and research institutions in France or abroad, or from public or private research centers.

L'archive ouverte pluridisciplinaire **HAL**, est destinée au dépôt et à la diffusion de documents scientifiques de niveau recherche, publiés ou non, émanant des établissements d'enseignement et de recherche français ou étrangers, des laboratoires publics ou privés.



## Open Archive Toulouse Archive Ouverte (OATAO)

OATAO is an open access repository that collects the work of Toulouse researchers and makes it freely available over the web where possible

This is an author's version published in: <http://oatao.univ-toulouse.fr/20344>

**Official URL:** <https://doi.org/10.1016/j.porgcoat.2015.03.024>

**To cite this version:**

Lassègue, Pierre and Noé, Laure and Monthieux, Marc and Caussat, Brigitte Iron deposition on multi-walled carbon nanotubes by fluidized bed MOCVD for aeronautic applications. (2015) physica status solidi (c), 12 (7). 861-868. ISSN 1862-6351

Any correspondence concerning this service should be sent to the repository administrator: [tech-oatao@listes-diff.inp-toulouse.fr](mailto:tech-oatao@listes-diff.inp-toulouse.fr)

# Iron deposition on multi-walled carbon nanotubes by fluidized bed MOCVD for aeronautic applications

Pierre Lassègue<sup>1</sup>, Laure Noé<sup>2</sup>, Marc Monthieux<sup>2</sup>, and Brigitte Caussat<sup>\*1</sup>

<sup>1</sup> LGC, ENSIACET-INP de Toulouse, UMR-5503 CNRS, 4 allée Emile Monso, BP 44362, 31432 Toulouse Cedex 4, France

<sup>2</sup> CEMES, UPR-8011 CNRS, 29 rue Jeanne Marvig, BP 94347, 31055 Toulouse Cedex 4, France

Received 2 March 2015, revised 7 May 2015, accepted 18 May 2015

Published online 8 June 2015

**Keywords** multi-walled carbon nanotubes, ferrocene, FB-CVD, ozone

\* Corresponding author: e-mail [brigitte.caussat@ensiacet.fr](mailto:brigitte.caussat@ensiacet.fr), Phone: +33 534 323 632, Fax: +33 534 323 697

The fluidized bed MOCVD process has been studied in order to uniformly deposit iron nanoparticles on the outer surface of multi-walled carbon nanotubes (MWCNTs) tangled in balls of 388  $\mu\text{m}$  in diameter. Using ferrocene as organometallic precursor at atmospheric pressure, various reactive atmospheres of deposition (under  $\text{N}_2$ , air and  $\text{H}_2$ ) and an ozone  $\text{O}_3$  surface pre-treatment of MWCNTs were tested. Around 10 g Fe/100 g MWCNTs were deposited during each run. Under  $\text{N}_2$  at 650  $^\circ\text{C}$  on the raw MWCNTs, nanoparticles formed of Fe and  $\text{Fe}_3\text{C}$  were deposited which have catalyzed the formation of

carbon nanofibers (CNFs). 20 h of ozone ( $\text{O}_3$ ) pre-treatment improved the number and distribution of iron nanoparticles but without increasing the surface coverage of nanotubes. A more intense amorphous carbon deposit also appeared. Under  $\text{H}_2$  at 550  $^\circ\text{C}$ , the amorphous carbon was partly eliminated but fewer iron nanoparticles were present. Under air at 450  $^\circ\text{C}$ , a part of the MWCNTs was lost and a  $\text{Fe}_2\text{O}_3$  shell covered each remaining MWCNTs ball. New works are in progress to increase more markedly the surface reactivity of MWCNTs and to deposit pure iron.

**1 Introduction** These last years, the aeronautic field is intensively looking for the mass reduction of planes to make them greener and more economical regarding fuel consumption. Their frame structure is today constituted of composite materials but it is not the case of the on-board electronic equipment packaging which is made of aluminum. To make this packaging lighter, new multifunctional composite materials need to be developed to replace aluminum while keeping its electrical and thermal evacuation capacities and mechanical properties in extreme conditions. Combination of carbon nanotubes (CNTs) and polymer matrix represents a promising alternative. CNTs are already used as reinforcement of polymers [1], but the final products do not exhibit a real improvement in its electrical and/or thermal behavior, despite the remarkable properties of CNTs in terms of conductivity [2, 3]. This work aims to improve the electrical and thermal conductivities of CNTs, and consequently those of the final composite material, by a metallic deposition of a continuous film or of homogeneously dispersed nanoparticles on their inert surface.

The metallization of CNTs is rapidly developing but most often by liquid solution methods, such as electroless deposition or liquid impregnation [4]. To produce in mass metallized CNTs, such technics would rapidly lead to large volumes of liquid effluents and then to strong environmental operating constraints and costs. Chemical Vapour Deposition (CVD) is a dry mode process which has been comparatively less studied for metallizing CNTs. Some works can however be found about the deposition of Pt [5], Ni [6] or Cu [7]. Some metalloids (Si [8]) and oxides ( $\text{TiO}_2$  [9] and  $\text{SnO}_2$  [10]) have also been deposited. The Fluidized Bed (FB) technology ensures a good mixing of the powder by the fluidization gas and then is an excellent contactor to perform CVD on multi-walled CNTs (MWCNTs) entangled as micro-balls [8]. The FB-CVD process is today the most efficient route to industrially produce MWCNTs by catalytic CVD [11]. So, developing a FB-CVD process for metallizing MWCNT balls would be economically and environmentally very interesting. To the best of our knowl-

edge, no work has been published about metal deposition on CNTs by FB-CVD.

Whatever the deposition method, the metals bind only weakly to the nanotube surface due to its chemical inertness [6]. Oxidation of CNTs by exposure to concentrated acids, in particular nitric acid ( $\text{HNO}_3$ ), is a popular functionalization method to increase their surface reactivity at the lab-scale [12]. Hydroxyl (C-OH), carbonyl (C=O) and/or carboxyl (O=C-OH) chemical groups can thus be formed, which additionally improves CNTs dispersion and interfacial behaviour with various polymer matrices [13]. However, the liquid wastes generated from these wet oxidation processes together with the tedious purification procedures would greatly limit their further development for industrial application [13]. Some works about gas phase oxidation of CNTs have been performed using either air [14, 15] or nitric acid vapours [16-18] at high temperature leading to mitigated results: the CNTs were structurally damaged or for worse partially burnt. The gas-phase oxidation from ozone ( $\text{O}_3$ ) is an environmental friendly and low cost route to form oxygen containing groups on the CNTs surface, even for mass production. Vennerbeg et al. [12] have successfully oxidized MWCNTs by an ozone/oxygen mixture in a lab-scale fluidized bed (containing 1 g of CNTs). After only a few tens of minutes of treatment, significant levels of oxidation (8 at.% O) were achieved with little damage to the nanotube sidewalls. Exposures of 60 min led to the formation of mainly carboxylic acid groups.

Iron is the first metal selected to coat MWCNTs in this study. It has good thermal ( $80.2 \text{ Wm}^{-1}\text{K}^{-1}$ ) and electrical ( $9.93 \times 10^6 \text{ Sm}^{-1}$ ) conductivities. Among the possible CVD precursors, iron pentacarbonyl  $\text{Fe}(\text{CO})_5$  presents a quite high volatility and is known to produce pure iron deposits [19, 20], but this precursor is highly toxic. This is the reason why it has not been chosen for our study. Iron trichloride  $\text{FeCl}_3$  presents a low volatility, needs high temperature ( $>600 \text{ }^\circ\text{C}$ ) to form iron films, and forms corrosive by-products [20]. A previous study of our group [21] aimed to deposit iron on alumina powders by FB-CVD. Two iron precursors have been compared, iron acetylacetonate  $\text{Fe}(\text{C}_5\text{H}_7\text{O}_2)_3$  or  $\text{Fe}(\text{acac})_3$  and ferrocene  $\text{Fe}(\text{C}_5\text{H}_5)_2$ . Various operating parameters have been tested, in particular two oxidative atmospheres,  $\text{N}_2$ +air and  $\text{N}_2$ + $\text{H}_2\text{O}$  vapor. The purest iron oxide deposits have been obtained using ferrocene under  $\text{N}_2$ +air, the deposits from iron acetylacetonate being always carbon contaminated. Moreover, ferrocene presents a higher volatility than  $\text{Fe}(\text{acac})_3$ , it is stable in air and non-toxic, quite cheap and easy to sublime to form stable vapour to feed the CVD reactor [22]. This explains why we have chosen to work with ferrocene. This precursor is also known to form carbon nanotubes [23, 24], but this formation can be controlled by modifying the reactive atmosphere. The addition of  $\text{H}_2$  is known to highly limit the formation of carbon products [25, 26]. As previously said, Philippe [21] has succeeded in depositing pure iron

oxide films using ferrocene under  $\text{N}_2$ +air. In a second step, these iron oxide films have been reduced under  $\text{H}_2$  at high temperature to form iron films.

In this framework, the present study aims to develop and optimize the FB-CVD process in order to uniformly coat the outer surface of MWCNTs by iron using ferrocene as precursor. Pristine and  $\text{O}_3$  treated MWCNTs have been studied in either inert ( $\text{N}_2$ ) or oxidant (air) or reductive ( $\text{H}_2$ ) CVD atmospheres.

**2 Experimental** Our experimental set up is presented in Fig. 1 and consists in a vertical stainless steel FB-MOCVD reactor (internal diameter of 8.3 cm and 1 m in height; reference (1) in Fig. 1) heated by a two-zone external furnace (2). At the bottom, a perforated steel plate (3) provides a homogeneous gas distribution. A high performance HEPA13 filtration cartridge (4) is mounted before the exhaust of the reactor to collect any elutriated particle. The ferrocene (Strem Chemicals) is used as received. It is loaded in a sublimator (5) placed in a thermostated oil bath and connected to the reactor entrance by a thermostated gas line. Gases ( $\text{N}_2$ , air and  $\text{H}_2$ ; Air Liquide) as well as ferrocene vapours are carried out to the bottom of the reactor. All of the gas lines are heated by silicon heater bands at the same temperature as the precursor sublimator to avoid any ferrocene condensation. Gas flows are controlled by mass flow meters (FC-7700 type; Aera) except for air which is controlled by a ball rotameter (GT1355; Brooks Instrument). A differential pressure sensor (Unik5000; Druck Ltd.) measures the total pressure drop across the MWCNTs bed. An absolute pressure sensor (PR21; Keller) allows monitoring the total pressure below the distributor. Temperature is monitored by several K-type thermocouples: three in a small tube along the vertical axis of the reactor to check the MWCNT bed isothermicity, two on the outer reactor walls to control the temperature furnace and one into the sublimator. The ozone generator (Lab2B, Ozonia) is connected to the bottom of the FB-CVD reactor and is fed with oxygen (Oxygen Alphagaz, Air Liquide), ensuring an ozone concentration of  $10 \text{ gh}^{-1}$  for a total gas flow rate of 10 slm. All the experiments are performed at atmospheric pressure.

Multi-walled carbon nanotubes (GRAPHIS-TRENGTH® C100; ARKEMA) are tangled in spherical balls of  $388 \mu\text{m}$  in Sauter diameter and look like black powder. Some amorphous carbon is present onto the walls and internal defects (compartments) are visible (Fig. 2). The wall number is between 5 and 15 and the external diameter between 7 and 15 nm. Their catalytic iron content is of 5.8 wt%. Their minimum fluidization velocity  $U_{\text{mf}}$  measured at ambient temperature under  $\text{N}_2$  is equal to  $1.2 \text{ cm s}^{-1}$ .

MWCNTs were analysed before and after ozone pretreatment and CVD by several characterization techniques. Thermogravimetric analysis (TGA) is performed in a thermobalance Q600 (TA Instrument) with a  $10 \text{ }^\circ\text{Cmin}^{-1}$  ramp from room temperature to  $1300 \text{ }^\circ\text{C}$  (estimation of the

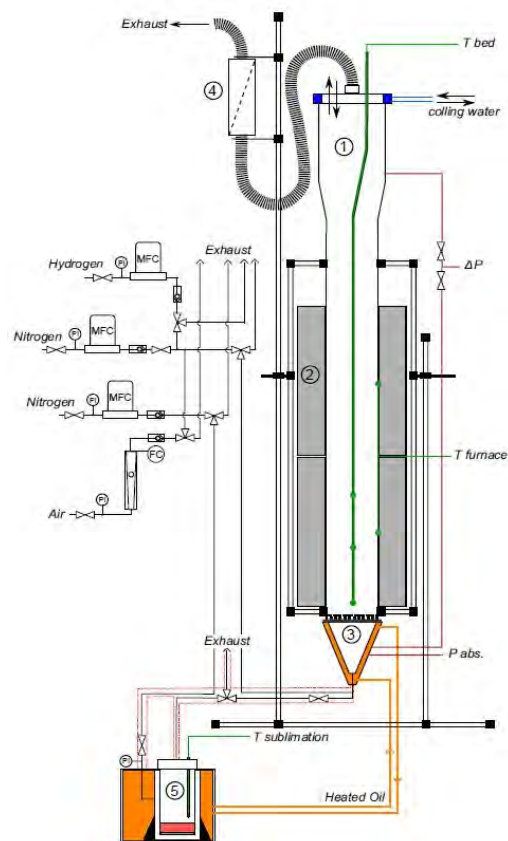


**Figure 1** Experimental set up.

**Table 1** Experimental CVD conditions.

Run	Type	Deposition temperature	Gas
1	Fe-N <sub>2</sub> -Raw	650 °C	N <sub>2</sub>
2	Fe-N <sub>2</sub> -O <sub>3</sub>	650 °C	N <sub>2</sub>
3	Fe-Air-Raw	450 °C	N <sub>2</sub> /Air
4	Fe-H <sub>2</sub> -O <sub>3</sub>	550 °C	N <sub>2</sub> /H <sub>2</sub>

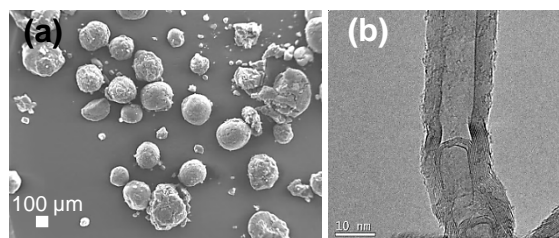


**Figure 2** (a) FEG-SEM view of the MWCNTs balls and (b) HRTEM view of a nanotube.

deposit mass) and to 1000 °C (qualitative analysis of the O<sub>3</sub> pre-treatment influence) under air and N<sub>2</sub> respectively. The powder morphology was observed by field emission gun scanning electron microscopy (FEG-SEM) on a Jeol JSM-7100F associated to an energy dispersive X-ray (EDX) detector (X-MAX<sup>N</sup> Oxford Instrument) and high resolution transmission electron microscopy (HRTEM) using a CM30 (Philips), LaB<sub>6</sub> gun and operated at 150 kV to minimise damaging irradiation effects. X-ray diffraction (XRD) results were obtained using a D8-2 (Drucker) with a monochromatic K $\alpha$  copper (Cu) source ( $\lambda = 1.5418 \text{ \AA}$ ). The operating conditions tested are detailed in Table 1. 100 g of MWCNTs were used for each experiment, corresponding to a ratio between the fixed bed height and the reactor diameter of 2.3. Such a ratio is necessary to ensure good thermal transfer between the reactor walls and the FB and then isothermal bed conditions which are well-suited for thermal CVD. The aim of the ozone treatment and of the CVD of iron is to uniformly treat the whole outer surface of MWCNT balls, i.e. to operate in kinetically-limited regime: the mass transport step of the reactive molecules through the porous media constituted by the bed and the MWCNTs balls must be more rapid than the chemical heterogeneous reaction step. The existence of this regime depends on numerous parameters, in particular the kinetics of the heterogeneous reactions, the surface reactivity of the powder and the operating conditions chosen. These parameters are difficult to *a priori* know for the present work. The ferrocene initial weight placed in the sublimator was fixed to 85 g.

### 3 Results and discussion

#### 3.1 MWCNTs pre-treatment by gaseous ozone

Ozone treatment in fluidized bed was applied during 20 h, with sampling after 1, 3, 9 and 20 h of treatment. TGA results under N<sub>2</sub> are presented in Fig. 3. The raw nanotubes are quite stable at temperatures up to 550 °C under N<sub>2</sub>. As observed by Kim and Min [13], the ozone treatment decreases the thermal stability of MWCNTs. The higher is the treatment duration, the lower is their thermal stability. After 1 h, the weight loss at 550°C is of 1.5 %, after 3 h, it reaches 2.1 %, whereas it stabilizes from 9 h at 4 %. These values are lower than those obtained by Kim and Min [13]. Vennerberg et al. [12] obtained up to 8 at% of grafted O in only 60 min, but both groups of authors use a larger concentration of O<sub>3</sub> per mass unit of CNTs. The weight loss observed is due to the escape of CO<sub>2</sub> gas produced during the oxidation of CNTs [13]. The analysis of the nature of the grafted functional groups is in progress using FT-IR and X-ray photoelectron (XPS) spectroscopies. The influence of ozonation on the MWCNTs structure has been analysed by HRTEM (Fig. 4). Only the MWCNTs treated during 20 h present external defects on their surface and amorphous carbon disappeared. For the shorter durations, no modification of the nanotube structure has been observed.

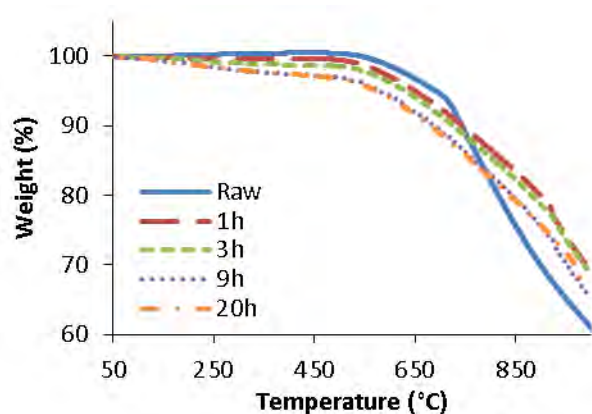


**Figure 3** TGA curves obtained under  $N_2$  showing the influence of the  $O_3$  treatment on the thermal stability of the MWCNTs.

### 3.2 Iron deposition under inert atmosphere with and without pre-treatment

*Without pre-treatment.* The target percentage of deposited Fe was of 10 g Fe/100 g MWCNTs in order to obtain reliable information from the various characterizations performed. Consequently, the ferrocene powder (85 g) was heated to 155 °C in the sublimator, leading to an inlet molar fraction of ferrocene close to 2.3%. The average bed temperature was fixed to 650 °C (see Table 1), higher than in the literature reports [23-27] for a better decomposition of the precursor. The total fluidization flow rate was of 5 slm, corresponding to a fluidization ratio  $U/U_{mf}$  of 4.

The experimental results are detailed in Table 2. Three different mass balances allow determining the gain in mass of the bed. The first one corresponds to a weighing of the bed before and after CVD. The second one consists in calculating the theoretical maximum iron mass which can be deposited onto the bed from the mass of sublimated ferrocene. The third one considers the pressure drop difference ( $\Delta P$ ) between the beginning and the end of deposition, knowing that if the bed remains conveniently fluidized,  $\Delta P$  is equal to the bed weight per column surface area. Table 2 indicates that from bed weighing and  $\Delta P$ , the gain in mass is equal to 57 g and 54 g respectively whereas from the precursor weighing, it is of 19.7 g. The good agreement between the two first balances means that the bed remained conveniently fluidized all along the deposition process. This was confirmed by the good isothermicity of the FB during deposition. The difference with the precursor balance implies that the deposit is not pure iron: about 34 to 37 g of the deposit could be formed of carbon or less importantly of oxygen (from ambient air) or hydrogen.

**Table 2** Mass balance and TGA results after CVD

Run	MWCNTs bed weight difference (g)	Max. Fe mass deposited from ferrocene sublimation (g)	Deposited mass on the bed from $\Delta P$ (g)	Iron wt% from TGA
1	57.0	19.7	54.0	8.5
2	52.5	22.0	55.2	10.7
3	-	20.7	-	-
4	37.8	19.4	35.9	8.3

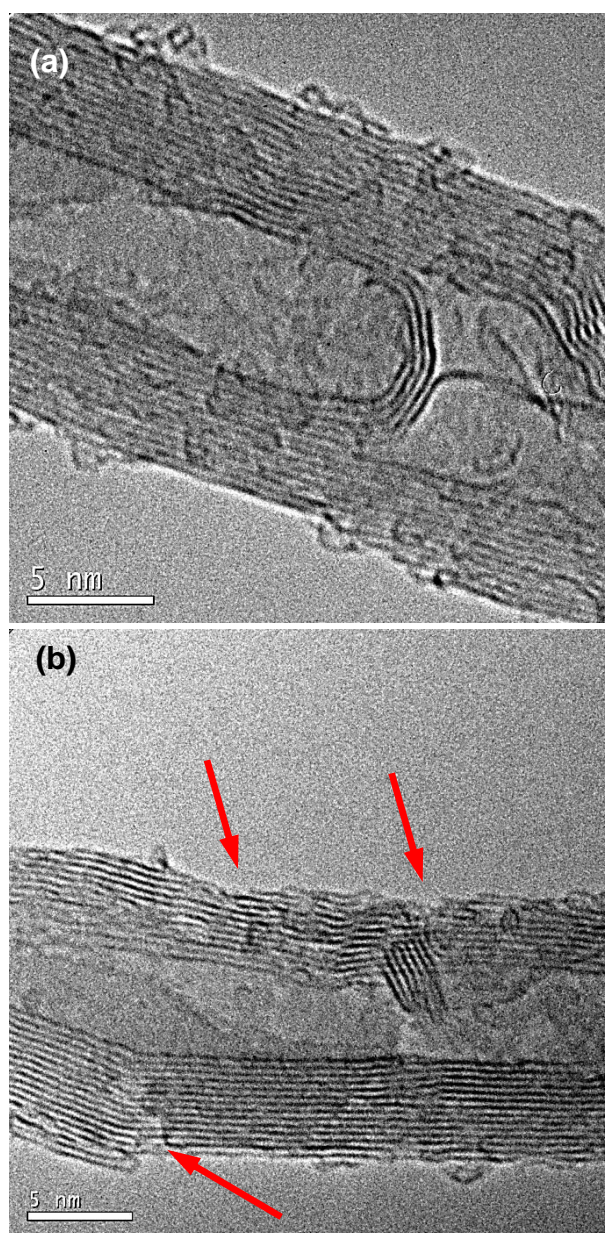


**Figure 4** HRTEM views of (a) raw MWCNT and (b) MWCNTs treated under  $O_3$  for 20 h; arrows represent structural defects on the surface after treatment.

TGA analyses under air (Fig. 5) show that 8.5 wt% of the bed is formed of iron (the initial iron catalyst mass (5.8 wt%) being removed). The target of 10 g Fe/100 g MWCNTs is almost reached. For the three iron deposition curves, the mass loss between 450 and 630 °C is due to the oxidation of the defects at the surface of the nanotubes and then to the nanotubes themselves. As Kim and Min [13] said, CO<sub>2</sub> is produced from O<sub>2</sub> and C of air and nanotubes respectively in higher quantity than for the TGA performed in inert atmosphere (Fig. 3). The small mass gain (~4 wt%) between 350 and 450 °C represents the oxidation of iron in Fe<sub>2</sub>O<sub>3</sub> [28]. The remaining 21 to 26 w%, assumed to be Fe<sub>2</sub>O<sub>3</sub>, has allowed to calculate the iron weight percentage in Table 2.

HRTEM observations show that the deposit occurred under the form of discrete particles whose size ranges from 50 to 500 nm (Fig. 6a). These particles are distributed everywhere in the MWCNT tangles but they have not uniformly covered the nanotube outer walls, as found by other authors about CVD of metals on CNTs [5-7]. They are covered by carbon layers and some of them have catalysed the post-formation of large, highly defective carbon nanofibers (CNFs) and nanotubes whose diameter is related to particle size, or alternatively are embedded in graphitic carbon shells (Fig. 6b). Ferrocene is indeed well-known to be a precursor of both iron and carbon nanomaterials [24]. The particles could then be saturated with carbon forming Fe<sub>3</sub>C and leading to CNF or CNT formation by CVD [29]. EDX cartography presented in Fig. 7, shows that iron is uniformly distributed both outside and inside the MWCNT balls, meaning that the kinetically-limited regime was reached under the conditions tested.

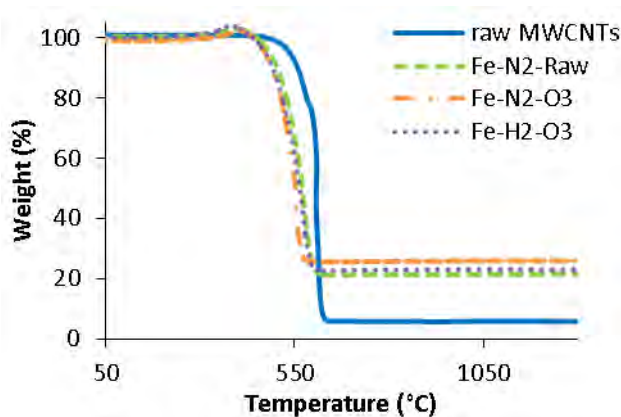


**Figure 5** TGA curves obtained under air of MWCNTs before and after CVD for the various conditions tested.

XRD analyses are presented in Fig. 8. The pristine MWCNT pattern shows three structural phases which are characteristic of the raw carbon nanotube material: 002<sub>C</sub> and 004<sub>C</sub> at 2θ = 25.8° and 51.7, respectively, which corres-

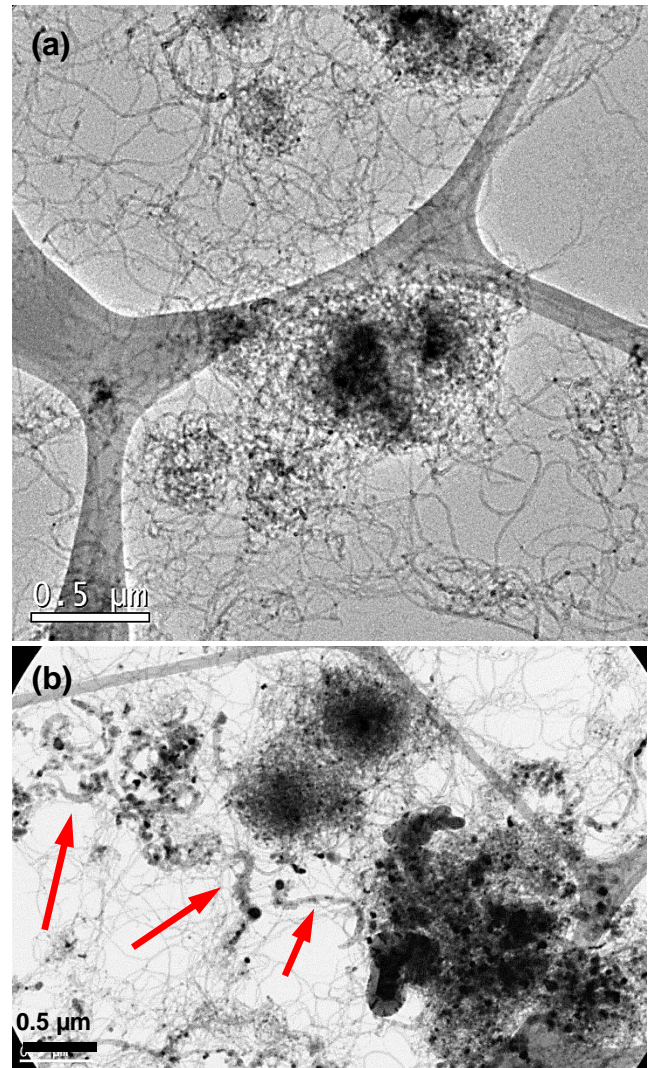


**Figure 6** HRTEM views of (a) raw MWCNTs and (b) WCNTs after run 1; arrows show CNFs formed after run 1.

pond to the first and second orders diffraction spots related to the inter-graphene stacking distance, and the 100<sub>C</sub> and 110<sub>C</sub> at respectively 42.7° and 78.2° which correspond to the in-plane periodicities of graphenes when stacked turbostratically. Hence, these peaks represent the chaotic tangle of the pristine MWCNTs observed by FEG-SEM previously. Still in the raw MWCNT pattern, two light shoulders could be attributed to iron and iron oxide signal (2θ = 44.5° and 48.5-49°, respectively): they originate from the initial catalyst used for the nanotube growth [8, 11]. The XRD pattern of the MWCNTs after CVD (inert atmosphere) reveals new peaks related to Fe<sub>3</sub>C at 2θ = 37.7°, 43.7° and 58° in accordance to the ICSD database. Additionally, iron signals at 44.5° and 49° form well-defined peaks. So, the deposit corresponds to a mixture of amorphous and structured carbon, pure iron and of iron carbide.

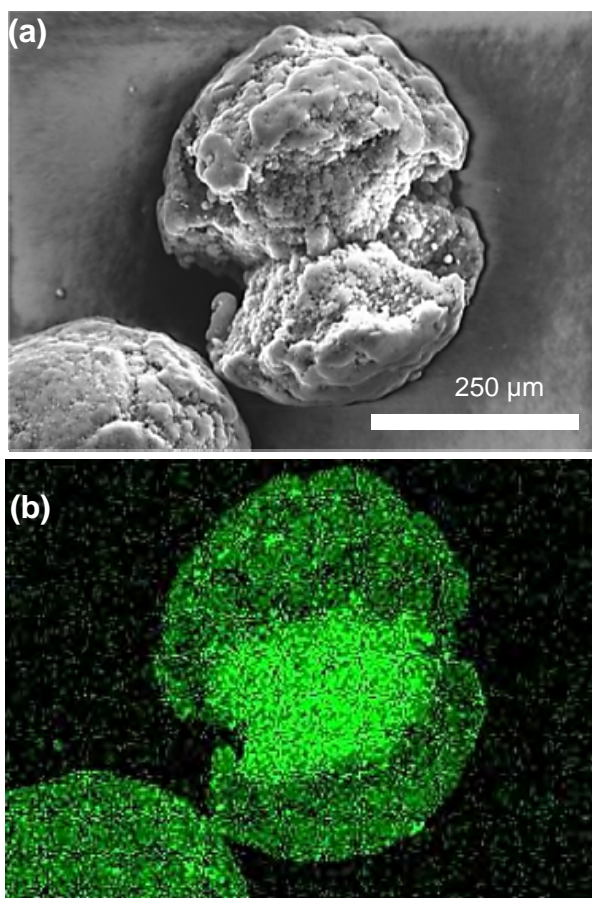


**Figure 7** (a) FEG-SEM view of an open MWCNT ball and (b) the corresponding EDX cartography of Fe (after run 1).

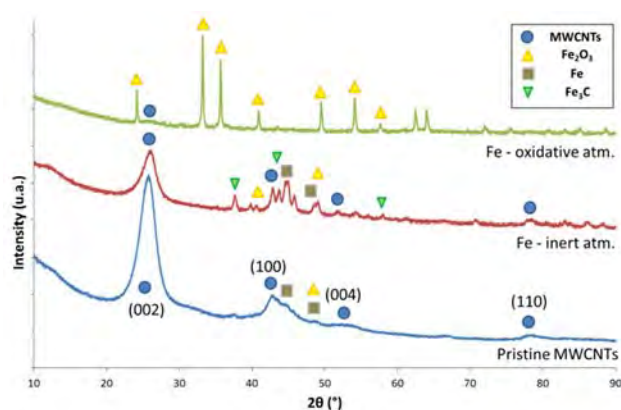


**Figure 8** XRD patterns of pristine (bottom) and CVD treated MWCNTs under  $N_2$  (middle) and air (top) without  $O_3$  pre-treatment of the MWCNTs.

*With pre-treatment.*  $O_3$ -treated MWCNTs were submitted to the same CVD conditions. The mass balances led to similar results: the masses of 52.5 g and 55.2 g were respectively deduced from MWCNTs weighing and  $\Delta P$  whereas the precursor mass balance gives 22 g, confirmed by TGA analysis (Fig. 5). The Fe percentage deduced from

TGA analysis is equal to 10.7 wt% (the initial iron catalyst content being removed) which means that the target of 10 g Fe/100 g MWCNTs is reached. So, the  $O_3$  treatment has increased by 2.2 % the mass of deposited iron. EDX analysis (not shown) indicates that iron is uniformly distributed everywhere in the MWCNT balls meaning that the kinetically-limited regime is still in place. HRTEM micrographs (Fig. 9) show the presence of amorphous carbon in larger amounts than before CVD. Indeed amorphous carbon is visible both around the deposited nanoparticles and on the MWCNTs outer walls and CNFs are still formed from the iron nanoparticles. The formed nanoparticles are still not covering the whole MWCNTs outer surface. They are smaller (10 to 100 nm) and at the HRTEM scale, more homogeneously distributed than those observed for pristine MWCNTs, which could be a possible positive effect of ozonation on the deposition. Indeed, ozonation could increase the number of nucleation sites by grafting oxygen containing groups on the outer MWCNT surface. The change of the MWCNT surface after ozonation seems to also modify the nature of the deposit in forming more amorphous carbon on the outer surface of MWCNTs, and maybe less carbon-contaminated iron nanoparticles. XRD and XPS analyses are in progress to confirm this point. This amorphous carbon could be partly responsible of the difference between the mass balances.

### 3.3 Iron deposition under oxidative atmosphere without pre-treatment.

The addition of air in the gas stream (30/70 vol% ratio of  $N_2$ /Air) aims to activate the decomposition of ferrocene in order to increase the deposit nucleation on the nanotube surface. If iron oxide nanoparticles would be deposited on the MWCNTs, they could be reduced after CVD to form iron nanoparticles. It has already been shown that MWCNTs can be burnt above 600 °C under oxidative atmosphere [30]. Thus, the temperature was decreased down to 450 °C. The other parameters remained unchanged (see Table 1).

Despite this precaution, half of the initial MWCNTs weight was oxidized and consumed during the experiment. The precursor mass balance gives 20.7 g of iron (see Table 2), showing the good reproducibility of the sublimation device. FEG-SEM micrographs show that the remaining MWCNTs balls are covered by a 10  $\mu m$  thick shell of deposit (Fig. 10a). As observed by Philippe et al. [11], the EDX cartography (Fig. 10b) reveals that this shell is mainly constituted of iron and oxygen and the XRD pattern (Fig. 8, top) confirms that it is hematite ( $Fe_2O_3$ ) (in accordance with the ICSD database). The core of the MWCNT balls is relatively depleted in iron. This indicates that the kinetically-limited regime was lost. A transport-limited regime has taken place instead: the activation of the heterogeneous chemical reactions by air was too intense and the reactivity of the MWCNT surface too low to lead to a uniform coating of each nanotube outer surface by iron oxide nanoparticles.

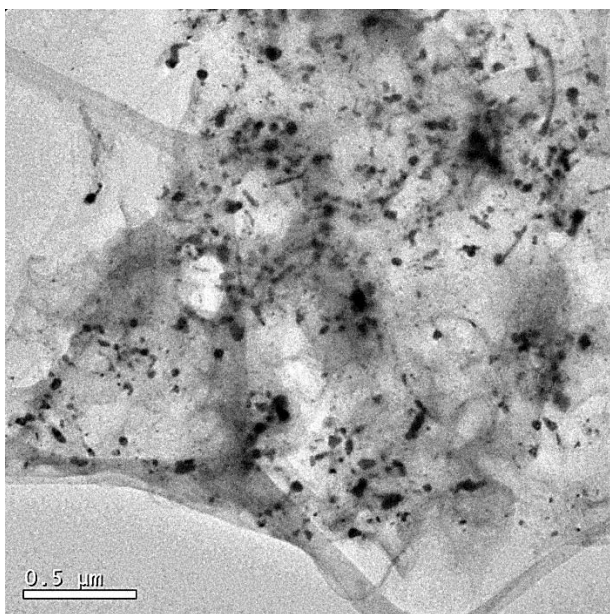


**Figure 9** HRTEM view of O<sub>3</sub>-MWCNTs after run 2 under inert atmosphere.

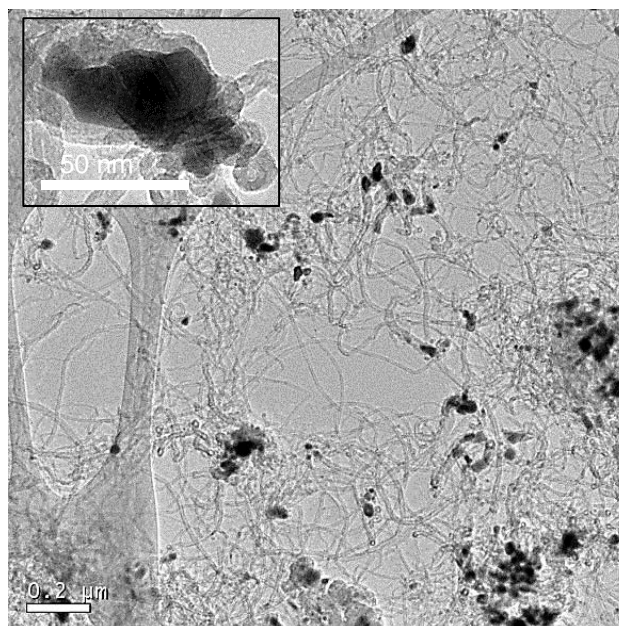


**Figure 11** HRTEM views of O<sub>3</sub>-MWCNTs after run 4 under reductive atmosphere; (sticker) zoom of a Fe nanoparticle covered by carbon layers but CNFs are absent.

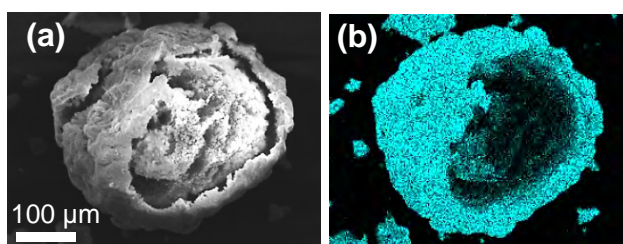


**Figure 10** (a) FEG-SEM view of a MWCNTs ball after run 3 under oxidative atmosphere and (b) its EDX cartography of Fe.

**3.4 Iron deposition under reductive atmosphere with pre-treatment** A N<sub>2</sub>/H<sub>2</sub> mixture was studied in order to prevent the formation of carbon nanofibers and of amorphous carbon previously observed for the experiments under inert atmosphere with O<sub>3</sub>-MWCNTs. It was previously shown that hydrogen is necessary to create MWCNTs but for a concentration higher than 23-27 vol%, the formation of carbon nanotubes is inhibited [25, 26]. Our N<sub>2</sub>/H<sub>2</sub> ratio was equal to 33/67 (vol%). The decomposition temperature of ferrocene under hydrogen is lower than under inert atmosphere [31, 32]. Consequently, the temperature for this run was decreased down to 550°C.

The mass balances deduced from MWCNT weighing and ΔP are lower than for run 2: 37.8 g and 35.9 g respectively whereas the precursor mass balance gives 19.4 g of iron. The Fe percentage deduced from TGA analysis is close to 8.3 wt% (the initial iron catalyst content being removed). So, these operating conditions reduce both the deposited weight and iron percentage in comparison with run 2.

HRTEM micrographs reveal the influence of H<sub>2</sub> (Fig. 11): amorphous carbon is still present around the deposited nanoparticles but it is now absent on the MWCNTs outer walls contrarily to run 2 under inert atmosphere. Moreover, the deposited nanoparticles are smaller than previously (size ranges between 20 and 50 nm). Although covered by carbon layers, they do not form anymore nanofibers. But they are, at the HRTEM scale, less numerous and less uniformly distributed. The presence of hydrogen and the lower temperature of deposition then reduce both carbon and less markedly iron deposition. Thus, the H<sub>2</sub> addition in the gas stream seems to have inhibited the formation of amorphous carbon and CNFs, as observed in the literature [25, 26].

**4 Conclusion** The fluidized bed CVD process was studied in order to uniformly decorate the outer surface of MWCNTs by iron deposits in a lab-scale reactor treating 100 g of nanotubes per run. An ozone treatment was also tested in the same fluidized bed reactor in order to increase the surface reactivity of nanotubes. TGA analyses reveal that oxygenated functions were grafted onto the surface of the MWCNTs in amounts proportional to the treatment duration, with a plateau observed from 9 h of treatment. After 20 h of ozonation, external defects were created on the surface of MWCNTs. Under N<sub>2</sub>/ferrocene atmosphere, for the pristine and O<sub>3</sub>-treated MWCNTs, the deposition occurs under the form of discrete particles uniformly distributed within the MWCNT balls. The ozone treatment increases the mass of deposited iron and the number of deposited nanoparticles and also decreases the size of the deposited

nanoparticles. This means that the ozonation increases the surface reactivity of the MWCNTs and the nucleation sites but not enough to uniformly cover the nanotube outer surface. Air was added to ferrocene in order to activate iron nucleation. A partial loss of the bed was observed at 450°C and Fe<sub>2</sub>O<sub>3</sub> shells were formed around the remaining MWCNT balls. Hydrogen was finally tested mixed to ferrocene at 550 °C, leading to less numerous nanoparticles deposited and also to less deposited amorphous carbon, without improving the surface coverage of the MWCNTs.

The main concern of the future works will be to increase much more markedly the surface reactivity of the MWCNTs. A possible way is to pre-treat MWCNTs by CVD of TiC [6]. Another way is to add water (H<sub>2</sub>O) vapour during the ozone pre-treatment [33]. Indeed, combined with O<sub>3</sub> at room temperature, water vapour seems to create HO· radicals and highly accelerate the ozonation [33]. Water vapour could also be added to ferrocene during iron deposition to eliminate carbon contamination [22]. The corresponding FB-CVD process on MWCNTs is under development.

**Acknowledgements** The authors thank Arkema for providing the MWCNTs and the SAP-LGC for characterization help. This work was financially supported by the Waspe FUI project and the Midi Pyrénées region.

## References

- [1] Z. Spitalsky, D. Tasis, K. Papagelis, and C. Galiotis, *Prog. Polym. Sci.* **35**, 357-401 (2010).
- [2] Q. Zhang, J. Q. Huang, W. Z. Qian, Y. Y. Zhang, and F. Wei, *Small* **9**, 1237-1265 (2013).
- [3] P. Kim, L. Shi, A. Majumdar, and P. L. McEuen, *Phys. Rev. Lett.* **87**, 215502-1 – 215502-4 (2001).
- [4] M. Monthieux, *Carbon Meta-Nanotubes: Synthesis, Properties and Applications* (Wiley-Blackwell, Chichester, 2012), p. 171
- [5] M. S. Saha, R. Li, and X. Sun, *J. Power Sources* **177**, 314-322 (2008).
- [6] M. Feng and R. J. Puddephatt, *Can. J. Chem.* **85**, 645-650 (2007).
- [7] C. Taschner, K. Biedermann, A. Leonhardt, B. Buchner, T. Gemming, and K. Wetzig, *Electrochem. Soc. Proc.* 396-402 (2005).
- [8] N. Coppey, L. Noé, M. Monthieux, and B. Caussat, *Chem. Eng. Res. Des.* **91**, 2491-2496 (2013).
- [9] S. Orlanducci, V. Sessa, M. L. Terranova, G. A. Battiston, S. Battiston, and R. Gerbasi, *Carbon* **44**, 2839-2843 (2006).
- [10] Q. Kuang, S. F. Li, Z. X. Xie, S. C. Lin, X. H. Zhang, S. Y. Xie, R. B. Huang, and L. S. Zheng, *Carbon* **44**, 1166-1172 (2006).
- [11] R. Philippe, B. Caussat, A. Falqui, Y. Kihn, P. Kalck, S. Bordère, D. Plee, P. Gaillard, D. Bernard, and P. Serp, *J. Catal.* **263**, 345-358 (2009).
- [12] D. C. Vennerberg, R. L. Quirino, Y. Jang, and M. R. Kessler, *ACS Appl. Mater. Interf.* **6**, 1835-1842 (2014).
- [13] J. H. Kim and B. G. Min, *Carbon Lett.* **11**, 298-303 (2010).
- [14] P. M. Ajayan, T. W. Ebbesen, T. Ichihashi, S. Iijima, K. Tanagaki, and H. Hiura, *Nature* **362**, 522-525 (1993).
- [15] K. Behler, S. Osswald, H. Ye, S. Dimovski, and Y. Gogotsi, *J. Nanopart. Res.* **8**, 615-625 (2006).
- [16] W. Xia, C. Jin, S. Kundu, and M. Muhler, *Carbon* **47**, 919-922 (2009).
- [17] C. Li, A. Zhao, W. Xia, C. Liang, and M. Muhler, *J. Phys. Chem. C* **116**, 20930-20936 (2012).
- [18] H. Rong, Z. Liu, Q. Wu, and Y. H. Lee, *Curr. Appl. Phys.* **10**, 1231-1235 (2010).
- [19] Y. H. Low, M. F. Bain, D. C. S. Bien, J. H. Montgomery, B. M. Armstrong, and H. S. Gamble, *Microelectron. Eng.* **83**, 2229-2233 (2006).
- [20] M. Corrias, Ph.D thesis, Nouvelle classe de catalyseurs pour la production massive en lit fluidisé de nanotubes de carbone multi-parois, Institut National Polytechnique de Toulouse, France, 2005.
- [21] R. Philippe, Ph.D thesis, Synthèse de nanotubes de carbone multi-parois par dépôt chimique en phase vapeur catalytique en lit fluidisé, Nouvelle classe de catalyseurs, étude cinétique et modélisation, Institut National Polytechnique de Toulouse, France, 2006.
- [22] F. Senocq, F. D. Duminica, F. Maury, T. Delsol, and C. Vahlas, *J. Electrochem. Soc.* **153**, G1025-G1031 (2006).
- [23] M. Lubej and I. Plazl, *Chem. Eng. J.* **242**, 306-312 (2014).
- [24] R. Bhatia and V. Prasad, *Solid State Commun.* **150**, 311-315 (2010).
- [25] W. Wasel, K. Kuwana, P. T. A. Reilly, and K. Saito, *Carbon* **45**, 833-838 (2007).
- [26] V. O. Nyamori, S. D. Mhlanga, and N. J. Coville, *J. Organomet. Chem.* **693**, 2205-2222 (2008).
- [27] A. Bhattacharjee, A. Rooj, D. Roy, and M. Roy, *J. Exper. Phys.* **2014**, 8 (2014).
- [28] M. Földvári, *Handbook of Thermogravimetric System of Minerals and its Use in Geological Practice* (Geological Institute of Hungary, Budapest, 2011), p. 179.
- [29] Q. Liu, Z. G. Chen, B. Liu, W. Ren, F. Li, H. Cong, and H. M. Cheng, *Carbon* **46**, 1892-1902 (2008).
- [30] N. Coppey, Ph.D thesis, Nanotubes de carbone décorés par CVD en lit fluidisé: Application en batterie lithium-ion, Institut National Polytechnique de Toulouse, France, 2013.
- [31] D. Qian, E. C. Dickey, R. Andrews, and D. Jacques, *Carbon* **1**, 1117-1119 (2001).
- [32] K. Kuwana and K. Saito, *Proc. Combust. Inst.* **31**, 1857-1864 (2007).
- [33] K. Peng, L. Q. Liu, H. Li, H. Meyer, and Z. Zhang, *Carbon* **49**, 70-76 (2011).